The 2019 World Congress on
Advances in Structural Engineering and Mechanics (ASEM19)
Jeju Island, Korea, September 17 - 21, 2019

Uniaxial compressive performance of RC columns with induced corrosion cracks

*Togo Aburano[1)], Amadou Sakhir Syll[2)] and Toshiyuki Kanakubo[3)]

[1),2)]*GSSIE, Univ. of Tsukuba, Ibaraki, 305-8573, Japan*
[3)]*Dept. of Eng. Mechanics and Energy, Univ. of Tsukuba, Ibaraki, 305-8573, Japan*
[1)] *s1920881@s.tsukuba.ac.jp*

ABSTRACT

The specific purpose of this study is to evaluate the influence of cover concrete cracks due to bar corrosion on the compressive performance of RC columns. The uniaxial compressive test was conducted using RC column specimens with induced corrosion cracks by aluminum pipe filled with an expansion agent. Induced cracks were obtained along aluminum pipe filled with an expansion agent and crack width tend to increase over elapsed time. From the test results, no significant correlation was found between induced cracks and the maximum compressive stress. No significant relationship was found between the coefficient expressing softening of cracked concrete and crack width. However, these results are in good agreements with those obtained in previous studies, when induced crack width is equal or superior to 0.3mm.

1. INTRODUCTION

A lot of reinforced concrete (RC) structures were built in the 1960s in Japan, and it is feared that these structures are damaged by bar corrosion. Today, many studies have researched on the relationship between bar corrosion and the performance of RC members. However, few studies are found out about the correlation between cover concrete cracks and the performance of RC members.

The previous study (Mogawa 2017) has suggested that the maximum stress of RC columns with induced corrosion cracks by electrolytic corrosion test is lower than the sound one. However, there were no significant relationship between clacks length and stress fallen after maximum stress. On the other hand, another study (Mogawa 2016) has suggested that slit length (=cracks length) and local destruction affect stress fallen after maximum stress using RC columns with induced corrosion cracks by slit. It is considered that more data are needed to evaluate the relationship between concrete

[1),2)] Graduate Student
[3)] Professor

cracks by bar corrosion and compressive performance of RC members.

Authors attempt to cause same crack as bar corrosion using an aluminum pipe filled with an expansion agent (Syll 2018). This method is able to cause cracks in short time compared to electrolytic corrosion test. It has been reported that the average crack width of RC beams using aluminum pipe filled with an expansion agent instead of compression bar was 0.5~1mm after 300 hours from filling it (Kawamura 2018).

The specific purpose of this study is to evaluate the influence of cover concrete cracks due to bar corrosion on the compressive performance of RC columns and specially to compare with the results of the previous study (Mogawa 2017) about stress fallen after maximum stress.

2. OUTLINE OF EXPERIMENT

2.1 Specimen

Table 1 shows the list of specimens, and Fig. 1 shows arrangement of bar. There are 15 specimens. Cross section is set as 250mm x 250mm and a test region is set as 250mm in middle of the height. Aluminum pipes with ϕ-18mm or ϕ-22mm are arranged in main bar position. An expansion agent is filled after 4 weeks later from concrete casting. Both ends of the specimen is reinforced by hoops (D6@30). The parameters are outer diameter of aluminum pipe, the number of pipes and elapsed time from filling an expansion agent to loading. Elapsed time is set 15, 65 and 300 hours as same as previous study (Syll 2018). It is supposed that elapsed time affects induced crack width.

Table 1 Specimens list

No.	Specimen ID	Outer diameter of pipe (mm)	Number of pipes	Elapsed time from filling to loading (h)
1	P18-N4-T15	18	4	15
2	P18-N4-T65		4	65
3	P18-N4-T300		4	300
4	P18-N8-NF		8	No agent
5	P18-N8-T15		8	15
6	P18-N8-T65		8	65
7	P18-N8-T300		8	300
8	P22-N4-NF	22	4	No agent
9	P22-N4-T15		4	15
10	P22-N4-T65		4	65
11	P22-N4-T300		4	300
12	P22-N8-NF		8	No agent
13	P22-N8-T15		8	15
14	P22-N8-T65		8	65
15	P22-N8-T300		8	300

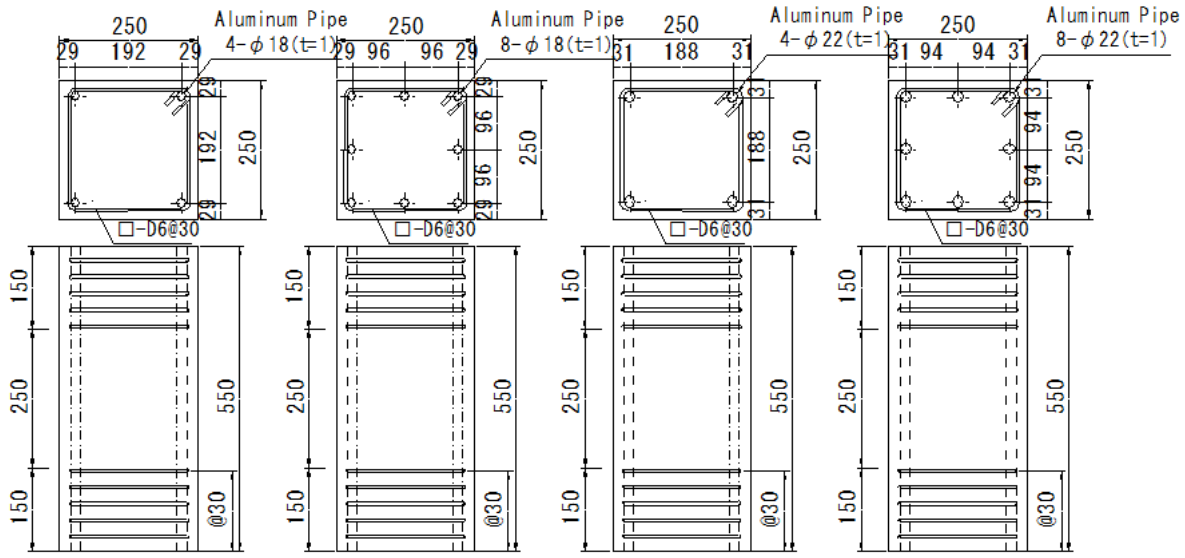

Fig. 1 Specimens

2.2 Material test result

Normal concrete that with 20mm maximum size aggregate was used. The target strength was 18MPa. Concrete was cast from the top of the specimen. According to the loading age of the column specimens, compression test was carried out three times using cylinder test pieces. These results are listed in Table 2. An aluminum pipe with ϕ-18mm or ϕ-22mm and 1mm thickness was used. Table 3 shows tension test results of the aluminum pipes. Axial and circumferential strains were measured, and Poisson's ratio was calculated. The listed results show the averages of three specimens.

Table 2 Mechanical property of concrete

Material age (day)	Compressive strength (MPa)	Elastic modulus (GPa)
41	19.2	25.2
47	16.7	23.4
51	17.6	22.9
Average	17.7	23.7

Tale 3 Mechanical property of aluminum pipe

Outer diameter	Tensile strength (MPa)	Yield strength (MPa)	Elastic modulus (GPa)	Poisson's ratio
18mm	230	211	66.9	0.342
22mm	218	198	64.3	0.333

2.3 Loading and measurement method

Fig. 2 shows loading and measurement method. Uniaxial compression loading was carried out using 2MN universal testing machine. For measuring axial deformation, π-type LVDTs were set on test region and LVDTs were set at the sides of the specimen. The deformation measured by π-type LVDTs was used until about 3mm deformation (1.2% strain), and thereafter the π-type LVDTs were removed. After that, axial deformation was obtained by deducting the difference between deformation measured by LVDT and that by π-type LVDTs at that time.

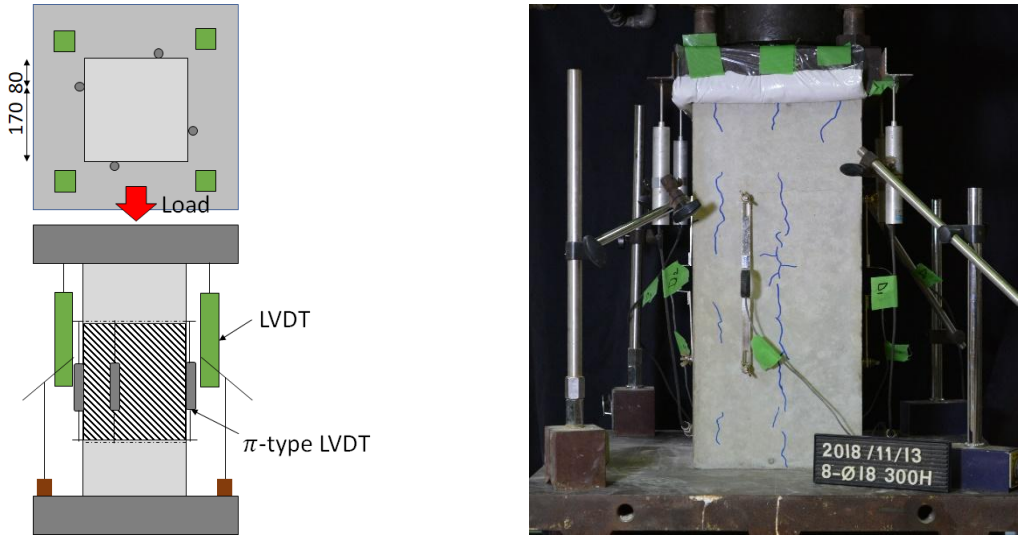

Fig. 2 Loading and measurement method

3. EXPERIMENTAL RESULTS

3.1 Cracks by expansion agent

Fig. 3 shows the examples of cracks, and Table 4 shows maximum crack width and average crack width before loading. The crack width that occurred along the pipe was measured using crack scale. In all specimens, crack was caused by expansion agent. The larger elapsed time tends to increase the maximum crack width and average crack width, and the difference between them also tends to increase. There was no significant relationship between the number of pipes and crack width. The crack length also increased as the elapsed time became long. In addition, the specimens with larger pipe outer diameter showed the larger crack width. Fig. 4 shows the transition of the maximum crack width by the elapsed time. In all specimens, the maximum crack width shows similar tendency until 50h from filling expansion agent. After that, the crack width in specimens with ϕ-18mm pipes tends to increase gradually, and that in specimens with ϕ-22mm pipes tends to increase suddenly.

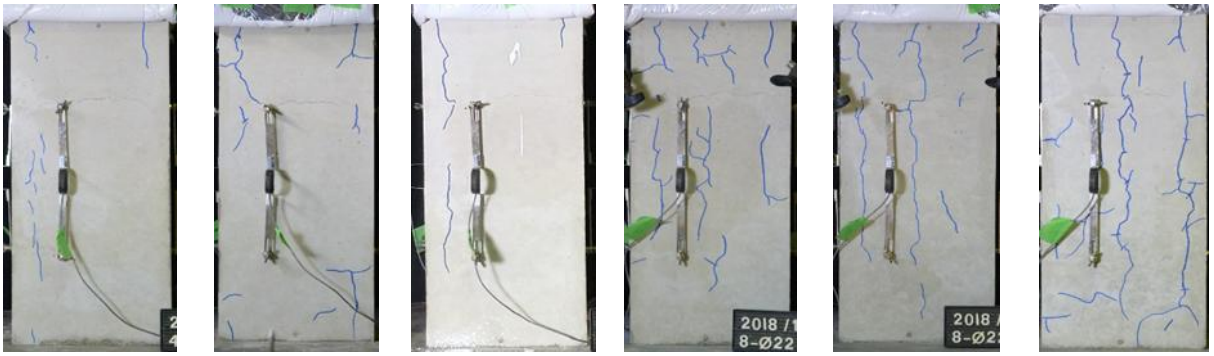

Fig. 3 Examples of specimens before loading

Table 4 The list of test results

Specimen ID	Crack width before loading (mm)		Maximum stress (MPa)	Strain at max. stress (%)
	maximum	average		
P18—N4-T15	0.08	0.05	14.56	0.257
P18-N4-T65	0.20	0.07	14.61	0.272
P18-N4-T300	0.40	0.20	15.41	0.262
P18-N8-NF	-	-	15.12	0.238
P18-N8-T15	0.10	0.05	14.93	0.197
P18-N8-T65	0.20	0.07	15.38	0.205
P18-N8-T300	0.40	0.07	15.25	0.253
P22-N4-NF	-	-	15.06	0.257
P22-N4-T15	0.05	0.05	14.89	0.300
P22-N4-T65	0.30	0.18	15.69	0.279
P22-N4-T300	0.90	0.58	14.50	0.183
P22-N8-NF	-	-	16.03	0.206
P22-N8-T15	0.05	0.05	15.66	0.228
P22-N8-T65	0.30	0.16	15.72	0.257
P22-N8-T300	0.80	0.25	16.00	0.298

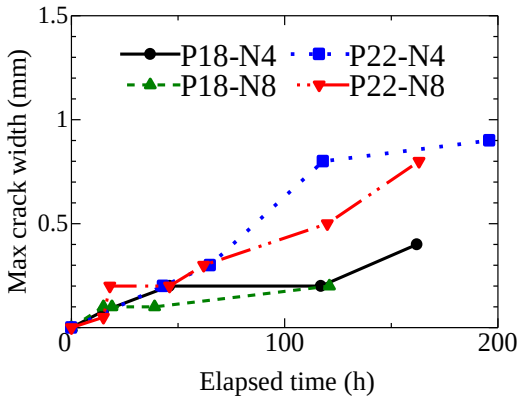

Fig. 4 Elapsed time vs. maximum crack width

3.2 Failure patterns in compression test

Fig. 5 shows the specimens after compression loading. In all specimens, cover concrete falling off, pipe buckling and damaged core concrete were observed. The specimens with 4 pipes tend to show cracks in the diagonal direction and the specimens with 8 pipes tend to show cracks in parallel to the pipes. In addition, transverse cracks in some pipes with ϕ-22mm diameter were observed due to buckling. No significant tendency in failure progress was found out by elapsed time.

Fig. 5 Examples of specimens after loading

3.3 Relationship between maximum stress and crack width before loading

Table 4 showed maximum stress and strain at maximum stress. Fig. 6 shows the relationship between maximum stress and crack width before loading. Stress was calculated by dividing compressive load by cross-sectional area (250mm x 250mm), and strain was calculated by dividing axial deformation by the length of test region. There is no significant relationship between maximum stress and crack width before loading. The maximum stress of specimens with ϕ-22mm pipes is larger than that of ϕ-18mm pipes. It is considered that the maximum stress is mainly affected by the compressive capacity of the pipes.

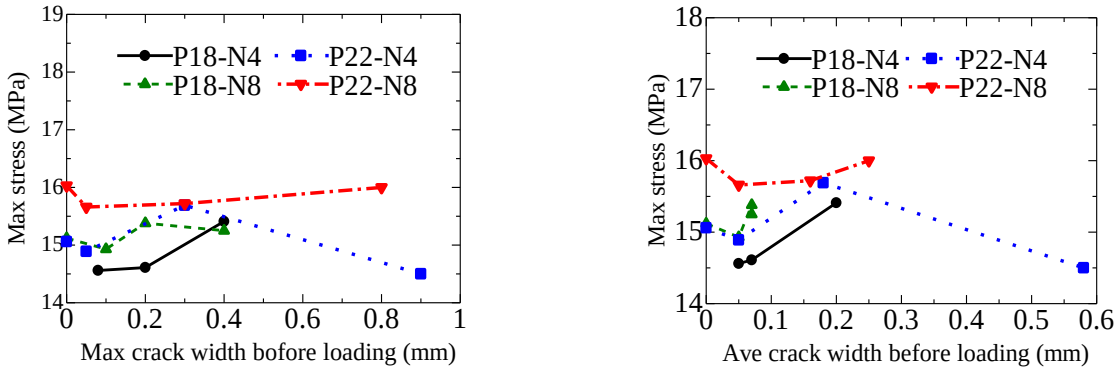

Fig. 6 Crack width before loading vs. maximum stress

3.4 Stress-strain curve

Fig. 7 shows the stress-strain curves, and Fig. 8 shows standardized stress-strain curves. Standardized stress-strain curve was calculated to focus on the softening curves after maximum stress. The larger elapsed time generally causes the softening curve gentler except for specimens of P18-N4 series.

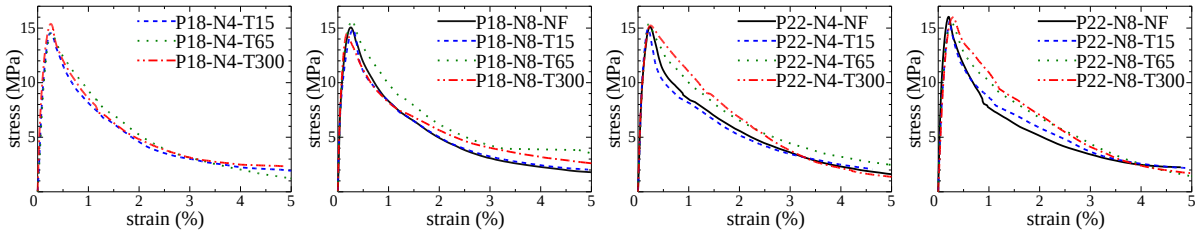

Fig. 7 Stress-strain curve

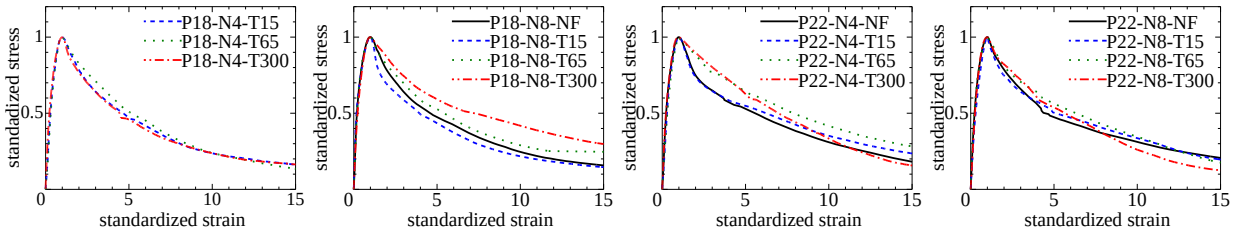

Fig. 8 Standardized stress-strain curve

4. EVALUATION OF SOFTENING GRADIENT OF CONCRETE

4.1 Calculation method of softening gradient

To calculate the softening gradient of concrete, concrete stress is obtained by substituting the stress carried by pipes from the total compressive load based on the assumption that plain section remains plain. The stress-strain curve of concrete is fitted by Popovics model (Popovics 1973) shown in Eq. (1) by the least square method using standardized stress-strain curve. The coefficient *n* in Popovics model expresses softening gradient.

$$\frac{\sigma}{\sigma_c} = \frac{n(\varepsilon/\varepsilon_c)}{n-1+(\varepsilon/\varepsilon_c)^n} \tag{1}$$

σ_c: maximum stress (MPa), ε_c: strain at maximum stress, *n*: coefficient

4.2 Compressive stress-strain model of pipe filled with expansion agent

The previous study (Syll 2018) reported compressive test results of pipes filled with expansion agent. These pipes have same diameter and thickness applied in this

study. Furthermore, elapsed time from filling expansion agent to loading are same with that in this study. The pipe filled with expansion agent are modeled assuming that the pipes similarly behaves even in concrete. Fig. 9 shows the compressive stress-strain curve of pipes filled with expansion agent. Up to maximum, the curve is modeled by the parabola shown in Eq. (2), and the softening branch is modeled by the straight line shown in Eq. (3). The maximum stress and the strain at the maximum stress were obtained as the average value of test results of 3 specimens. The slope of the softening line of each specimen was obtained by the least square method. Table 5 shows the coefficient *m* that express the slope of softening and Fig. 9 also includes the models.

$$\sigma_p = \sigma_{max}\{2\,\varepsilon/\varepsilon_{max} - (\varepsilon/\varepsilon_{max})^2\} \tag{2}$$

$$\sigma_p = \sigma_{max}\left(1 - \frac{\varepsilon - \varepsilon_{max}}{2m\,\varepsilon_{max}}\right) \tag{3}$$

σ_{max} : maximum stress (MPa), ε_{max} : strain at maximum stress *m*: coefficient

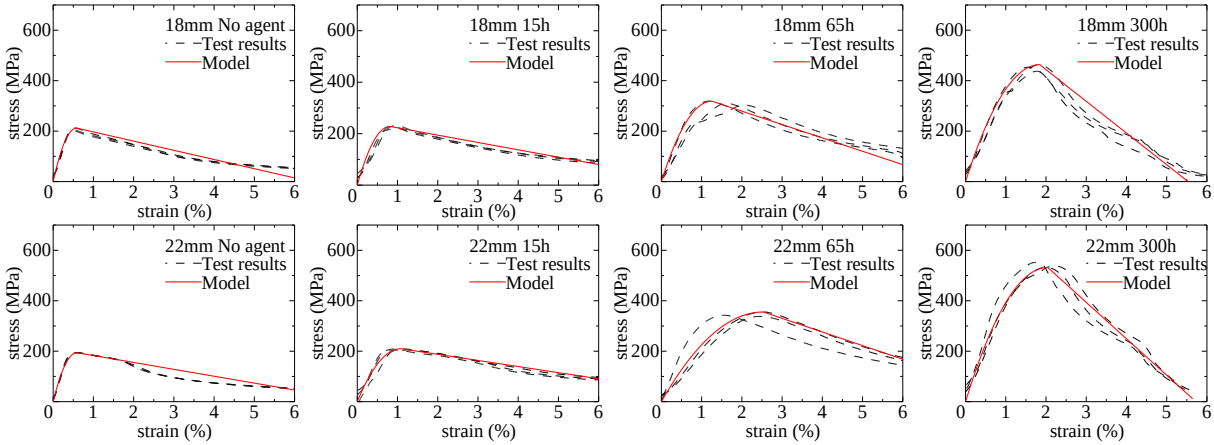

Fig. 9 Stress-strain curve of pipes filled with expansion agent

Table 5 Compressive model of pipes filled with expansion agent

Outer diameter	Elapsed time (h)	*m*	Outer diameter	Elapsed time (h)	*m*
18mm	No agent	5.0	22mm	No agent	6.0
	15	4.9		15	4.0
	65	2.4		65	1.3
	300	1.0		300	0.9

4.3 Softening gradient of concrete

Table 6 shows the maximum stress of concrete and evaluated values for *n*. Maximum stress has no significant relationship with crack width before loading as similar with that shown in Fig. 6. Fig.10 shows the examples of standardized stress-strain curve of concrete comparing fitted models. The previous study (Mogawa 2016) reported that the range of *n* was 1.75~3.48. Except for the specimens of P18-T300 series, it is recognized that the number of pipes increases, the value of *n* also increases, i.e., softening gradient tends to be large. There is no significant influence on the value of *n* by outer diameter and elapsed time. Fig. 11 shows the relationships between *n* and maximum crack width and average crack width before loading. Focusing on the specimens of P22-N8 series, the larger crack width brings the larger *n*. However, in other specimens, no relationship is observed. Table 7 shows the list of *n* and crack length ratio that proposed in the previous study (Mogawa 2016). Crack length ratio is defined as the total crack length divided by the test region length. The relationship between the crack length ratio and *n* has been evaluated by Eq. (4). In this study, cracks with a half or more of test region length are assumed to be those took place in the entire test region. The calculated values of *n* by Eq. (4) do not agree with experimental values, and the errors are large.

$$n = \frac{0.13(L_{cr}/L)+1.81}{(L_f/L)^{0.84}} \tag{4}$$

n: coefficient, L_{cr}: crack length (mm), L: test length (mm), L_f: length of local failure of concrete (mm), in this study, it is assumed that there is no local failure (L_f/L=1).

A 0.5mm thick polypropylene sheet was used to simulate crack in the previous study in which Eq. (4) was derived. Therefore, it is assumed that cracks with a width of less than 0.3mm have no effect in this study. Table 7 lists the errors between the calculation results and experimental value. The calculated results using the cracks equal or more than 0.3mm wide show smaller errors.

Table 6 List of maximum stress of concrete and evaluated values for *n*

ϕ-18mm	Max. stress (MPa)	*n*	ϕ-22mm	Max. stress (MPa)	*n*
-	-	-	P22-N4-NF	14.17	1.87
P18-N4-T15	14.20	1.99	P22-N4-T15	14.05	1.89
P18-N4-T65	14.49	1.90	P22-N4-T65	14.95	1.80
P18-N4-T300	15.04	2.02	P22-N4-T300	14.02	1.84
P18-N8-NF	14.66	1.93	P22-N8-NF	15.23	1.93
P18-N8-T15	14.71	2.13	P22-N8-T15	15.13	2.03
P18-N8-T65	15.21	1.91	P22-N8-T65	15.28	2.00
P18-N8-T300	14.82	1.87	P22-N8-T300	14.96	2.23

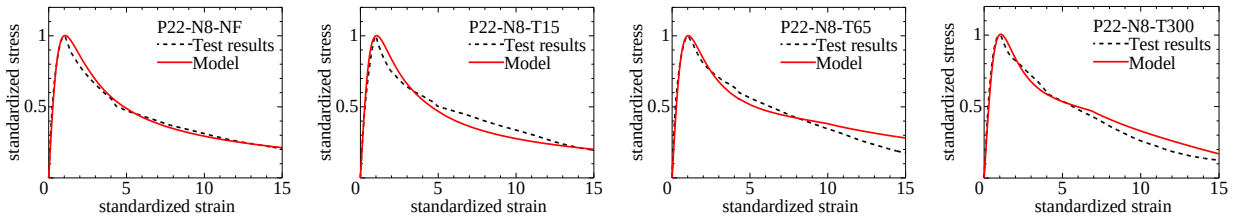

Fig. 10 Example of fitted model

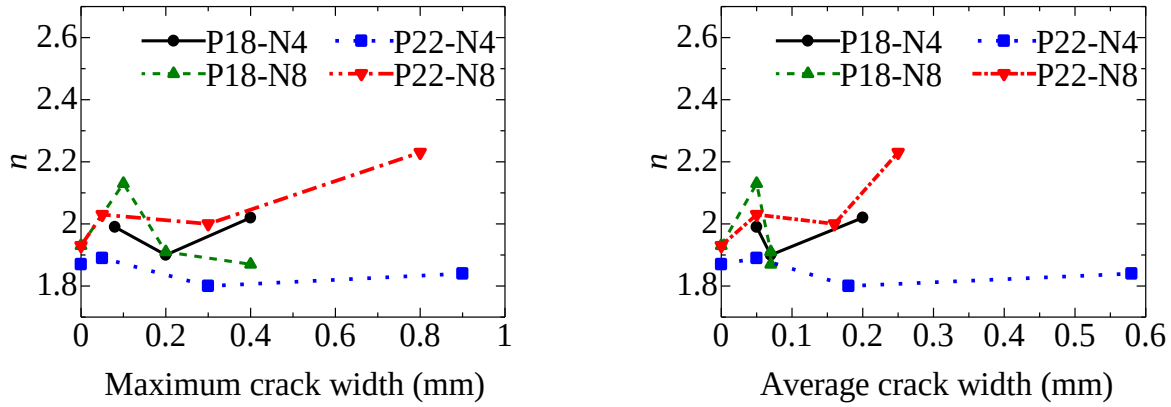

Fig. 11 Crack width before loading vs. *n*

Table 7 List of crack length ratio and calculated *n*

Specimen name	*n* Test results	Crack length ratio	Calculated *n*	Error (%)	Crack length ratio (0.3mm over)	Calculated *n*	Error (%)
P18-N4-T15	1.99	2	2.07	4	0	1.81	9
P18-N4-T65	1.90	4	2.33	23	0	1.81	5
P18-N4-T300	2.02	6	2.59	28	1	1.94	4
P18-N8-NF	1.93	0	1.81	6	0	1.81	6
P18-N8-T15	2.13	2	2.07	3	0	1.81	15
P18-N8-T65	1.91	8	2.85	50	0	1.81	5
P18-N8-T300	1.87	7	2.72	46	0	1.81	3
P22-N4-NF	1.87	0	1.81	3	0	1.81	3
P22-N4-T15	1.89	-	-	-	0	1.81	4
P22-N4-T65	1.80	6	2.59	44	2	2.07	15
P22-N4-T300	1.84	6	2.59	41	4	2.33	27
P22-N8-NF	1.93	0	1.81	6	0	1.81	6
P22-N8-T15	2.03	5	2.46	21	0	1.81	11
P22-N8-T65	2.00	10	3.11	56	2	2.07	4
P22-N8-T300	2.23	12	3.37	51	6	2.59	16

5. CONCLUSIONS

In this study, the uniaxial compressive test was conducted using RC columns specimens with induced corrosion cracks by aluminum pipe filled with expansion agent and the influence of cover concrete cracks due to bar corrosion on the compressive performance of RC columns was evaluated. The larger elapsed time after filling the expansion agent tends to increase the maximum crack width and average crack width. There is no significant relationship between induced cracks formulation and maximum stress obtained by compression test. The softening gradient of concrete has also no influence by the crack width before loading, the number of cracks, and crack length. Experimental results expressing the softening gradient of concrete show good agreements with calculated value, when induced cracks of equal or more than 0.3mm wide are considered.

REFERENCES

Mogawa, T., Kanakubo, T., Yasojima, A., Oyado, M. (2016), “Uniaxial Compressive Performance of RC Columns with Simulated Cracks due to Corrosion”, *Int. C. Asian Concrete Fed.*, Paper No. **44**

Mogawa, T., Kanakubo, T., Yasojima, A., Oyado, M. (2017), “Uniaxial Compressive Performance of RC Columns with Simulated Cracks due to Corrosion”, *Proceedings of the Japan Concrete Institute*, Vol. 39, No.**2,** 140-150 (in Japanese)

Syll, A. S., Kawamura, Y., Kanakubo, T. (2018), “Simulation of Concrete Cracks due to Bar corrosion by Aluminum Pipe Filled with An Expansion Agent”, *Summaries of Technical Papers of Annual Meeting, AIJ*, Structure IV, 55-56

Kawamura, Y., Kanakubo, T. (2018), “Flexural Performance of RC Beams with Simulated Cracks due to Bar Corrosion by Aluminum Pipe Filled with An Expansion Agent”, *Conference of Kanto Branch of JSCE*, V-22 (in Japanese)

Popovics, S. (1973), “A Numerical Approach to the Complete Stress-Strain Curve of Concrete”, *Cement Concrete Research*, Vol.**3**, 583-599